ISSN 1028-334X, Doklady Earth Sciences, 2020, Vol. 494, Part 1, pp. 748–752. © Pleiades Publishing, Ltd., 2020.
Russian Text © The Author(s), 2020, published in Doklady Rossiiskoi Akademii Nauk. Nauki o Zemle, 2020, Vol. 494, No. 1, pp. 91–96.

PHYSICS OF ATMOSPHERE

# Analysis of Trends in Aridity Changes for the Southern Ural Region over the Period 1960–2019 Using Various Methods

**D. Yu. Vasilev[a,b,*], V. V. Vodopianov[a],**
**Corresponding Member of the RAS V. A. Semenov[b,c,d], and Academician A. A. Chibilev[e]**

Received July 1, 2020; revised July 3, 2020; accepted July 3, 2020

**Abstract**—A statistical analysis of extreme episodes of aridity and humidity for the territory of the Southern Urals was performed. The calculations were based on the average daily air temperature and daily precipitation from 11 stations over the period 1960–2019. The spatial temporal characteristics of the summer droughts were studied on the basis of the station observations and calculated quantitative parameters. It has been established that the frequency of droughts in the Southern Ural region has increased over the past 19 years, the spread of the phenomenon reaches its peak in July.

**Keywords:** precipitation, air temperature, extreme drought, extreme moisture, climate variability
**DOI:** 10.1134/S1028334X20090214

Over the past several decades, global climate change has led to significant imbalances in hydrothermal conditions in natural ecosystems in many regions of the Earth. As a consequence of this, droughts [1], which are caused by a lack of moisture, are becoming increasingly frequent [2]. As the intensity, frequency, and duration of droughts has increased, this trend has become one of the most serious issues for many countries around the world [3–5]. In accordance with the official statistics of the World Meteorological Organization (*https://public.wmo.int/ru*), hydrometeorological disasters represent 70% of the total number of natural disasters; droughts are estimated to be responsible for half of all those disasters. The increase in the num-

**Table 1.** The main characteristics of the observation network used

| Meteorological station (synoptic code) | Geographical coordinates | | Elevation of the meteorological site, m |
|---|---|---|---|
| Yanaul (28419) | 56°16′ N | 54°58′ E | 98 |
| Kushnarenkovo (28624) | 55°05′ N | 55°20′ E | 98 |
| Aksakovo (28719) | 54°01′ N | 54°08′ E | 358 |
| Ufa (28722) | 54°42′ N | 54°48′ E | 104 |
| Tukan (28823) | 53°50′ N | 57°29′ E | 551 |
| Sterlitamak (28825) | 53°36′ N | 55°56′ E | 136 |
| Sorochinsk (53011) | 52°26′ N | 53°08′ E | 102 |
| Zilair (35026) | 52°14′ N | 57°27′ E | 522 |
| Orenburg (35121) | 51°45′ N | 55°06′ E | 109 |
| Akbulak (35127) | 51°01′ N | 55°38′ E | 143 |
| Dombarovskii (35223) | 50°47′ N | 59°32′ E | 276 |

[a] *Ufa State Aviation Technical University, Ufa, 450008 Russia*
[b] *Obukhov Institute of Atmospheric Physics, Russian Academy of Sciences, Moscow, 119017 Russia*
[c] *Institute of Geography, Russian Academy of Sciences, Moscow, 119017 Russia*
[d] *Institute of the Steppe, Ural Branch, Russian Academy of Sciences, Orenburg, 460000 Russia*
[e] *Institute of Water Problems, Russian Academy of Sciences, Moscow, 119333 Russia*
**e-mail: vasilevdy@ugatu.su*

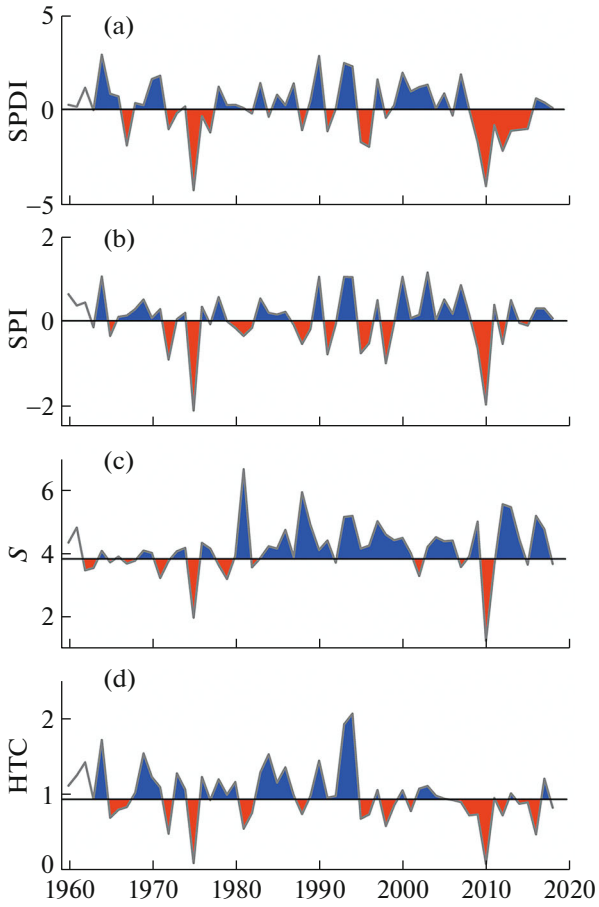


**Fig. 1.** The periods of (red) droughts and (blue) humidity in the Southern Urals over the period of 1960–2019: (a) SPDI, (b) SPI, (c) Ped index, and (d) Selyaninov index.

ber and duration of droughts has led to significant change in the spatial temporal distribution of humidity of the territories. The purpose of this work is to study the spatial temporal trends in the aridity changes through the example of the Southern Urals. A great number of indicators can be used to analyze the spatial temporal features of aridity/humidity. They are generally divided into two groups, single indicators and multiple indicators. The first ones generally characterize the dynamic of droughts on the basis of the main factor, which, as a rule, is precipitation. The second group of indicators takes into consideration a great number of physical parameters, which involve, besides precipitation, data on evaporation, air temperature, soil moisture, etc.

**Table 2.** Correlation analysis of the temporal series of the aridity indexes over the period of 1960–2019

| Index | HTC | *S* | SPI | PDSI |
|---|---|---|---|---|
| Selyaninov | **1** | 0.33 | **0.79** | **0.69** |
| Ped | 0.33 | **1** | 0.32 | 0.22 |
| SPI | **0.79** | 0.32 | **1** | **0.80** |
| PDSI | **0.69** | 0.22 | **0.80** | **1** |

Note. Statistically significant values of the Pearson's correlation coefficient $r$ at a level of $p = 0.001$ at $n = 60$ are indicated in bold.

In hydrometeorological practice, the most commonly used aridity indexes are the following:

The Ped Index $S$ [6] is the difference between the standardized values of air temperature anomalies $t$ and atmospheric precipitation $P$:

$$S = T/\sigma(T) - \Delta P/\sigma(P), \quad (1)$$

where σ is the mean square deviation of the mean values of temperature and precipitation.

The Selyaninov Hydrothermal Coefficient (HTC) or Selyaninov Index [7] is generally calculated as the ratio of the total precipitation $R$ to the sum of active temperatures $T$ (an indicator characterizing the active vegetation phase of agricultural crops) reduced ten times for the same periods of time:

$$\mathrm{HTC} = R/0.1\sum T. \quad (2)$$

The Palmer Drought Severity Index (PDSI) [8] has the final formula

$$\mathrm{PDSI}_i = 0.897\mathrm{PDSI}_{i-1} + Z_i/3, \quad (3)$$

where $i$ is the time range, as a rule, a month; $Z$ is the Palmer index of the moisture anomaly, which is calculated as

$$Z = Kd, \quad (4)$$

where $K$ is the weighted climatic indicator and parameter $d$ is the difference between the total atmospheric precipitation and the water-balance equation.

The Standardized Precipitation Index (SPI), which is calculated by means of transformation of data on atmospheric precipitation to the normal (Gaussian) distribution, where the mean value of the index over the period considered is equal to zero and the mean square deviation is equal to one [9].

The indexes were calculated using the mean daily data on the surface temperature and the total daily atmospheric precipitation over the period from 1960 to 2019. The data were obtained from the Unified State Fund of the Federal State Budgetary Institution All-Russia Research Institute of Hydrometeorological Information-World Data Center (RIHMI-WDC), Roshydromet (http://www.meteorf.ru) from 11 meteorological stations located in the Southern Ural region. Table 1 shows the basic characteristics of the station network used in this work. The related computational procedures for the aridity index determinations were carried out in [10]; after that, the aridity index arrays for the Southern Urals were formed [11] and averaged for the desired area, similarly to what was done in [12, 13].

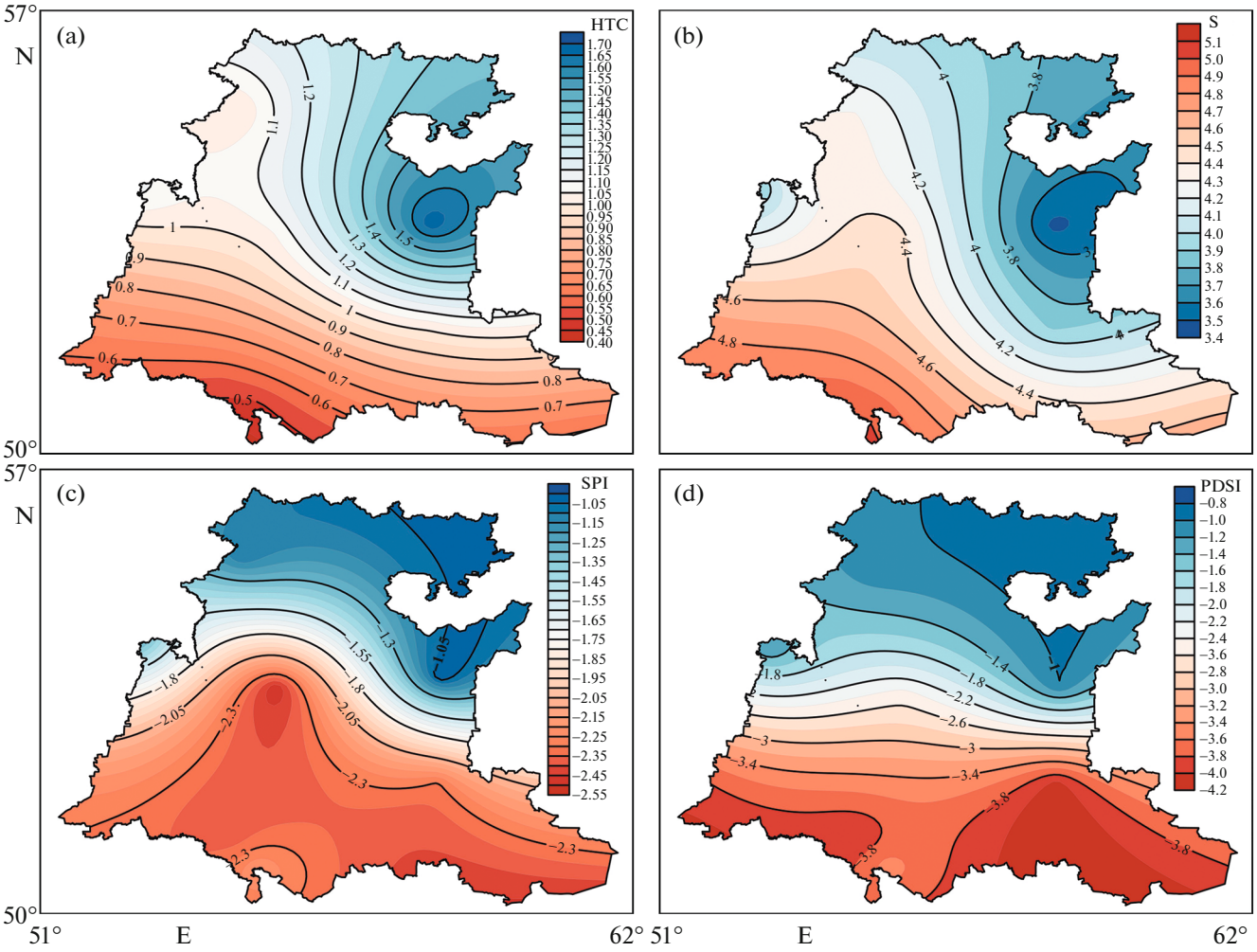


**Fig. 2.** The spatial distribution of the aridity indexes over the period of 1960–2019: (a) Selyaninov index, (b) Ped index, (c) SPI, and (d) PDSI.

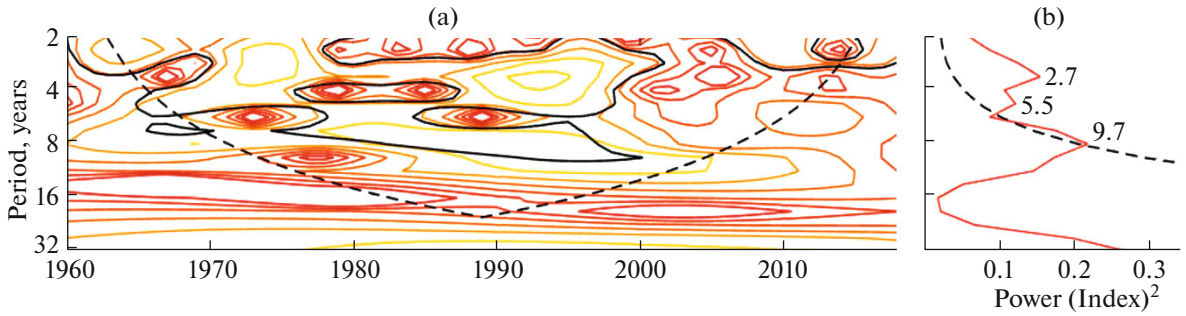


**Fig. 3.** The wavelet analysis of the Selyaninov index (HTC): (a) local spectrum, (b) power spectrum. A border of 95% statistical significance and the respective cone of influence are indicated by the dashed line.

The key finding of this study is the aridization the Southern Ural region over the past several decades. All four aridity indexes for the summer season clearly showed two of the most dramatic cases of extreme droughts in 1975 and 2010. In Fig. 1, the periods of extreme aridity are shown with deep red; a blue color indicates the areas of extreme humidity. Blocking anticyclones were the main reasons for these catastrophic phenomena. Under the influence of these anticyclones, hot and dry weather with the preceding abnormally cold winter, which caused deep soil freezing, was observed in the Southern Ural region. There-

**Table 3.** Classification of droughts on the basis of the Selyaninov Index [7]

| Drought type | HTC |
|---|---|
| Excessive humidity or drainage zone | more than 1.3 |
| Sufficient humidity | 1.0–1.3 |
| Dry | 0.7–1.0 |
| Dry agriculture | 0.5–0.7 |
| Irrigation | less than 0.5 |

fore, most of the atmospheric precipitation of the winter–spring period was transformed into stream flow, thereby accelerating the beginning drought. The long-term dry periods, which were observed over the past 19 years, are related to the changes in the interannual distribution of atmospheric precipitation, namely, an increase in the share of the fall–winter precipitation in comparison with precipitation of the spring–summer season.

Figure 2 shows the areal visualization, which was made for the spatial estimation of all four indexes. The distribution of the arid zones and zones with excessive humidity is similar for all four indexes on the territory of the Southern Urals. The wetlands involve the mountain–forest region and some areas of the forest–steppe zone. Drier lands occupy most of the forest–steppe zone, the steppe zone, and the Trans-Urals. The distribution of the aridity/humidity areas is explained by the features of the physical geography of the Southern Urals, primarily, the barrier effect of the Ural Mountains, the presence of large highlands, and latitudinal zoning on the Earth in general.

On the basis of impartial analysis, it is important to establish which index of the four calculated is the most suitable for the study area. For this purpose, comparative and correlation analyses were conducted. The results of the correlation analysis are represented in Table 2. The highest value of the Pearson's correlation coefficient was revealed for the Selyaninov Hydrothermal Coefficient in comparison with all three aridity indexes.

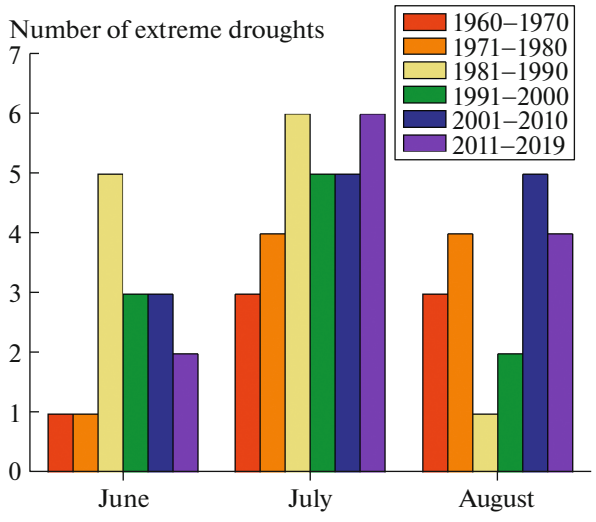


**Fig. 4.** The histograms of the extreme droughts during the summer season for separate months and climatic periods indicated in the Southern Urals.

The comparative analysis was based on comparison of the extreme values of the aridity indexes and the instrumentation data of the surface meteorology. This analysis showed results similar to those obtained by the correlation analysis. Therefore, the further frequency–temporal analysis was conducted only on the basis of the Selyaninov Index. The frequency–temporal analysis itself was based on calculations of the main statistical characteristics and the wavelet transform (Fig. 3), similarly to [14, 15].

A quasi-ten-year harmonic is a dominant and statistically significant cycle on the temporal interval represented. Figure 3b clearly shows the global power spectrum of the analyzed signal on an index periodogram. To reveal the trends in HTC variations, further comparisons of the variability were made for the decades taking into consideration this result. In our case, the 60-year series of data on the Selyaninov Index was divided into six quasi-ten-year periods (I, from 1960 to 1970; II, from 1971 to 1980; III, from 1981 to 1990; IV, from 1991 to 2000; V, from 2001 to 2010; and VI, from 2011 to 2019). Then, the calculated values of the Selyaninov Index were rated on the basis of the generally accepted hydrometeorological practice of the Selyaninov Index gradations [7], which is represented in Table 3. The values of the Selyaninov Index, which are equal to 0.6 or less, were selected. These values are equivalent to extremally dry conditions for the summer season as a whole and for the three warm months separately. The results of this selection are represented in diagrams in Fig. 4, where a decrease in aridity in June and August and an increase in aridity in July for the Southern Ural region are observed. Generally, during the summer season, there is a trend toward an increased number of droughts.

In conclusion let us note that the spatial–temporal analysis with the use of the aridity indexes of Selyaninov, Ped, SPI, and PDSI allowed us to provide a complex estimation of the humidity dynamics for the territory of the Southern Urals. A strong close relation between the Selyaninov index and the other aridity indexes was established. This made it possible to use the Selyaninov index to solve the problems on analyzing droughts and humidity conditions and to forecast climate change. The analysis showed that the Selyaninov index adequately represents the aridity and humidity for the Southern Ural region from 1960 to 2019. It was established that, over the past 19 years, the number of droughts generally increased in July and over the summer period; however, in June and August,

aridization decreased. The results of this study may be used for validation of climatic models and long-term forecasting.

## ACKNOWLEDGMENTS

The authors are grateful to the Bashkir Directorate for Hydrometeorology and Environmental Monitoring; the Orenburg Center for Hydrometeorology and Environmental Monitoring; the Privolzhskii Department for Hydrometeorology and Environmental Monitoring; Roshydromet; and V.Z. Gorokholskaya and M.S. Utesenova for providing the long-term data on the basic meteorological characteristics.

## FUNDING

This work was supported by the Russian Science Foundation, project no. 19-17-00242. The data processing and calculation of indexes were carried out according a State Assignment, project no. 0148-2019-0009.

## REFERENCES

1. O. A. Drozdov, *Droughts and Humidification Dynamics* (Gidrometeoizdat, Leningrad, 1980) [in Russian].
2. *IPCC, 2013: Climate Change 2013: The Physical Science Basis. The Working Group I contribution to the Fifth Assessment Report of the Intergovernmental Panel on Climate Change (IPCC),* Ed. by T. F. Stocker and D. Qin (IPCC, Cambridge, New York, 2013).
3. A. N. Zolotokrylin, E. A. Cherenkova, and T. B. Titkova, Izv. Ross. Akad. Nauk, Ser. Geogr. **84** (2), 207–217 (2020).
4. D. N. Utkuzova, V. M. Han, and R. M. Vil'fand, Atmos. Oceanic Opt. **28** (4), 336–347 (2015).
5. W. Li, L. Duan, W. Wang, Y. Wu, T. Liu, Q. Quan, X. Chen, H. Yin, and Q. Zhou, Meteorol. Atmos. Phys. (2020). https://doi.org/10.1007/s00703-020-00727-4
6. D. A. Ped', Tr. Gidromettsentra SSSR, No. 156, 19–38 (1975).
7. G. T. Selyaninov, Tr. S-kh Meteorol., No. 20, 165–177 (1928).
8. B. Lloud-Hughes and M. A. Saunders, Int. J. Climatol. **22** (13), 1571–1592 (2002).
9. *Standardized Precipitation Index. User Guide* (WMO, 2012), Vol. 1090, p. 18.
10. D. Yu. Vasil'ev, V. V. Vodop'yanov, A. K. Kostetskii, and V. A. Semenov, PC Software Certificate No. 2020616448 (17.06.2020).
11. D. Yu. Vasil'ev, V. V. Vodop'yanov, A. K. Kostetskii, and V. A. Semenov, Data Base Certificate No. 2020620991 (17.06.2020).
12. D. Yu. Vasil'ev, O. K. Babkov, I. R. Davliev, V. A. Semenov, and O. I. Khristodulo, Opt. Atmos. Okeana **31** (4), 294–302 (2018).
13. D. Yu. Vasil'ev, N. V. Velikanov, V. V. Vodop'yanov, N. N. Krasnogorskaya, V. A. Semenov, and O. I. Khristodulo, Issled. Zemli Kosmosa, No. 2, 14–28 (2019).
14. D. Yu. Vasil'ev, R. L. Lukmanov, Yu. I. Ferapontov, and A. N. Chuvyrov, Dokl. Earth Sci. **448** (1), 131–135 (2013).
15. D. Yu. Vasil'ev, V. M. Pavleichik, V. A. Semenov, J. T. Sivohip, and A. A. Chibilev, Dokl. Earth Sci. **478** (5), 245–250 (2018).

*Translated by V. Krutikova*